Coastal Geomorphic Responses to Sea Level Rise: Galveston Bay, Texas

Stephen P. Leatherman

INTRODUCTION

This chapter describes the geomorphic effects of projected sea level rise on low-lying coastal landforms along southeast Galveston Bay, Texas, for a range of Projected sea level rise rates (baseline, low, medium and high) at particular time periods (2025 and 2075). The objective is to determine the coastal changes in response to various assumed sea level increases by these particular dates. Two categories of physical response are addressed: shoreline changes representing landward displacement of the land/water interface and changes in storm surge levels and inland inundation as a result of the projected rates of sea level rise. Groundwater changes, resulting from saltwater intrusion coastal aquifers, were originally considered (Leatherman et al., 1983), but sea level rise was found to result in minimal effects compared to those of cultural alterations. For instance, the groundwater supplies in the Galveston area have already been polluted or overexploited. Also, land surface subsidence, largely resulting from overpumping, has been so pronounced that legislation has recently been enacted prohibiting the further development of groundwater resources (Thompson, 1982).

A section of Galveston Island and Bay was selected for this pilot study (see Figure 5-1). This portion of the Gulf coastal plain is quite low and gently seaward. Therefore, a slight rise in sea level would result in, significant horizontal displacement of the shoreline and storm surge envelope. Other selection criteria included microtidal environment, major Gulf Coast estuary, highly developed population centers and industrial complexes at Texas City and north Galveston Island, availability of the National Weather Service storm surge model SLOSH (Sea, Lake and Overland Surges from Hurricanes), and information on historical erosional trends and subsidence data.

Three sea level rise scenarios were developed (see Chapter 3); eight rise/year combinations were selected from the projected sea level rise curves for this analysis (see Table 5-1). The table indicates, for example, that absent any acceleration in sea level rise (the baseline scenario), by 2025 sea level will have risen by 13.7 cm (0.5 ft). In the medium sea level rise scenario, sea level will have risen by 48.4 cm (1.6 ft) in 2025. Although subsidence has been a major problem in Texas City, the estimated rate of future subsidence for this area is insignificant, with Galveston Island being essentially stable (Thompson, 1982).

As indicated in Figure 5-1, the Galveston study area was divided into several subareas. The results of this analysis are given in tables for all subareas. Graphic representations are presented for illustrative purposes in order to conserve space.

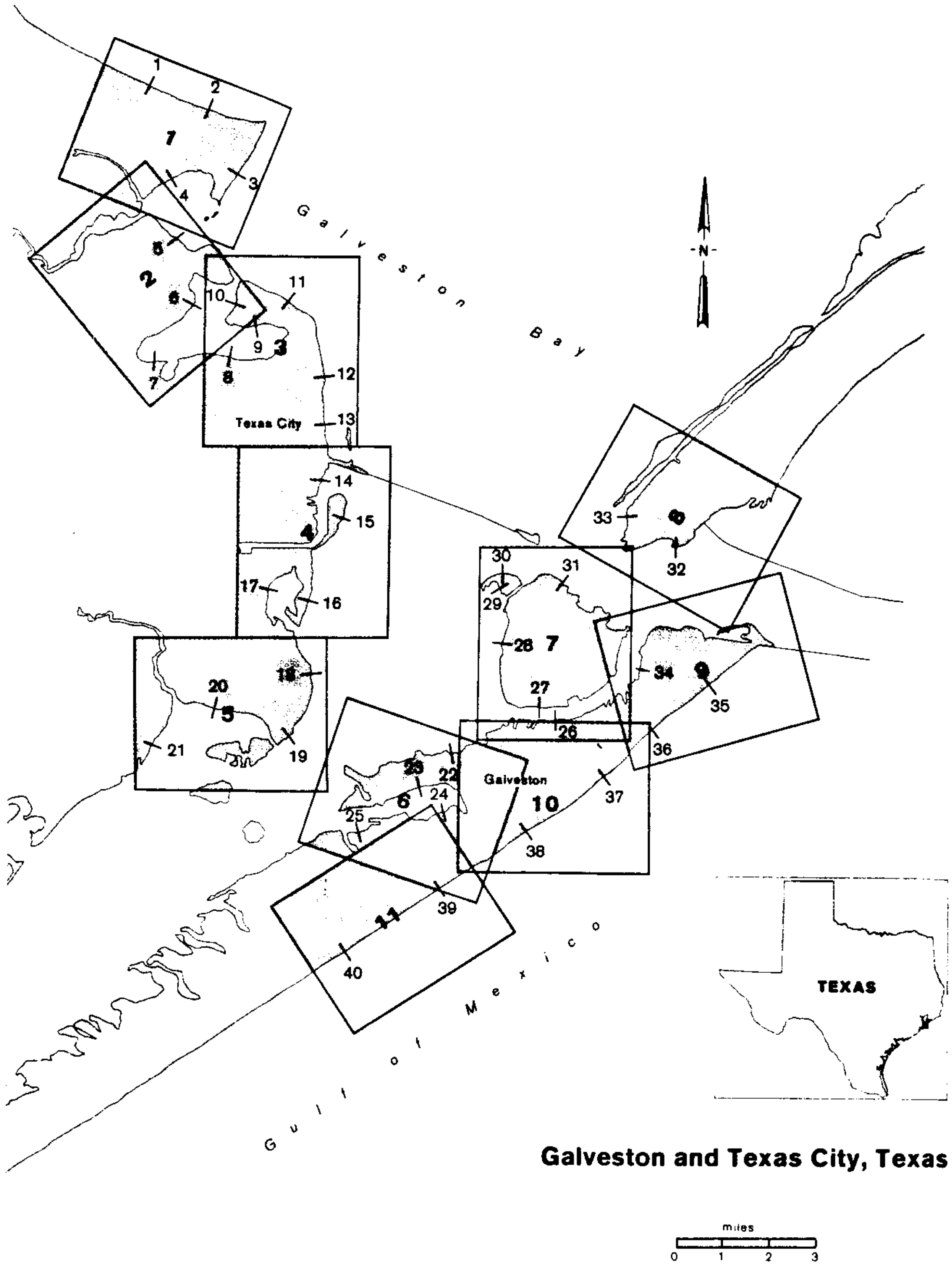

Figure 5-1. Index map showing relative location of 11 shoreline map sections.

Figure 5-1. Index map showing relative location of 11 shoreline map sections.

Table 5-1. Accelerated Sea Level Rise Scenarios for Galveston (in cm, with ft in parentheses)

Scenario	Year 1980	2025	2075
Baseline	0	13.7 (0.5)	30.0 (1.0)
Low	0	30.7 (1.0)	92.4 (3.0)
Medium	0	48.4 (1.6)	164.5 (5.4)
High	0	66.2 (2.2)	236.9 (7.8)

Table 5-1. Accelerated Sea Level Rise Scenarios for Galveston.

Coastal zones are inherently dynamic environments, being characterized by differing geomorphic processes and coastline configurations. To account for this wide variability in site and process, this study has combined analyses of historical trends and empirical approaches to model projected changes in the Galveston Bay area associated with the sea level rise scenarios. Shoreline changes are the major example of the former approach. Former shoreline positions portrayed on historical maps, once digitized and transformed by a sophisticated shoreline mapping program (metric mapping; Leatherman, 1983), form the basis for projecting potential shoreline excursion rates as a result of sea level rise. These extrapolated rates were assessed in light of possible impacts that recent human modification-such as levees and seawalls-may have on future trends. Empirical models have been used to derive baselines for changes in storm surge inundation. Results of the SLOSH model for the Galveston Bay area provide a base for predicting changing flood levels for each respective sea level scenario. The following sections discuss the impacts of sea level rise on shoreline retreat and storm surge levels, followed by discussions and general conclusions.

SHORELINE RESPONSE

Sea level rise has been identified as the principal forcing function in shoreline retreat along sandy coasts worldwide (Bird, 1976). As sea level rises, a number of complex and related phenomena come into play. Rising sea levels (transgression) are accompanied by a general retreat of the shoreline. This is produced by erosion or inundation. Erosion is the physical removal of beach and cliff material, while inundation is the submergence of the otherwise unaltered shoreline.

Figure 5-2 illustrates the combined effects of erosion and submergence due to sea level rise. The term D_I represents the landward movement of the shoreline due to simple inundation of the land; the response time is instantaneous. Therefore, direct submergence of the land occurs continuously through time and is particularly evident in coastal bays where freshwater upland is slowly converted to coastal marshlands (termed upland conversion).

The second displacement term (D_2) refers to a change in the profile configuration according to Bruun (1962). The Bruun Rule provides for a profile of equilibrium in that the volume of material removed during shoreline retreat is transferred onto the adjacent shoreface/inner shelf, thus maintaining the original bottom profile and nearshore shallow water conditions (only further inland). Figure 5-3 is a more accurate depiction of this two-dimensional approach of sediment balancing between eroded and deposited quantities in an on/offshore direction. Hands (1976) found that the Bruun Rule was confirmed by actual field surveys of beach profiles during rising lake levels on Lake Michigan. The volume of sand eroded from the beach nearly matched the offshore deposition.

Beach stability in a two-dimensional sense (Bruun Rule) should theoretically be reached; W.

Seelig (1982) has shown that beach equilibrium can be achieved under wave tank conditions.[1] Perhaps a constructive way of viewing the allied roles of sea level position and sea energy (coastal storms) is to consider that sea level sets the stage for profile adjustments by coastal storms. Long-term sea level rise places the beach/nearshore profile out of equilibrium, and sporadic storms accomplish the geologic work in a quantum fashion. Major storms are required to stir the bottom sands at great depths offshore and hence fully adjust the profile to the existing water level position. Therefore, the underlying assumption is that beach equilibrium will be the result of water level position in a particular wave climate setting.

Shore response lag times are tied to storm intensity and frequency, as shown by Hands (1976). The lag time in shoreline response to lake level was shown to be rather short (approximately 3 years). This rapid response time is due to the fact that the Great Lakes are subject to frequent storm activity in the fall/winter before surface icing.

Along the Gulf of Mexico, sea energy is quite low except during hurricane conditions. Tropical storms are sporadic in behavior and can only be dealt with in a statistical manner (recurrence interval-a frequency,/magnitude approach). Therefore, Galveston Island, for example, may be considerably out of adjustment with sea level changes over an extended period of time before being affected by a major hurricane ($\leq$ 15 years). This analysis suggests that each area will have a different lag time in shoreline response depending upon the local storm frequency, which must be treated in a probabilistic fashion.

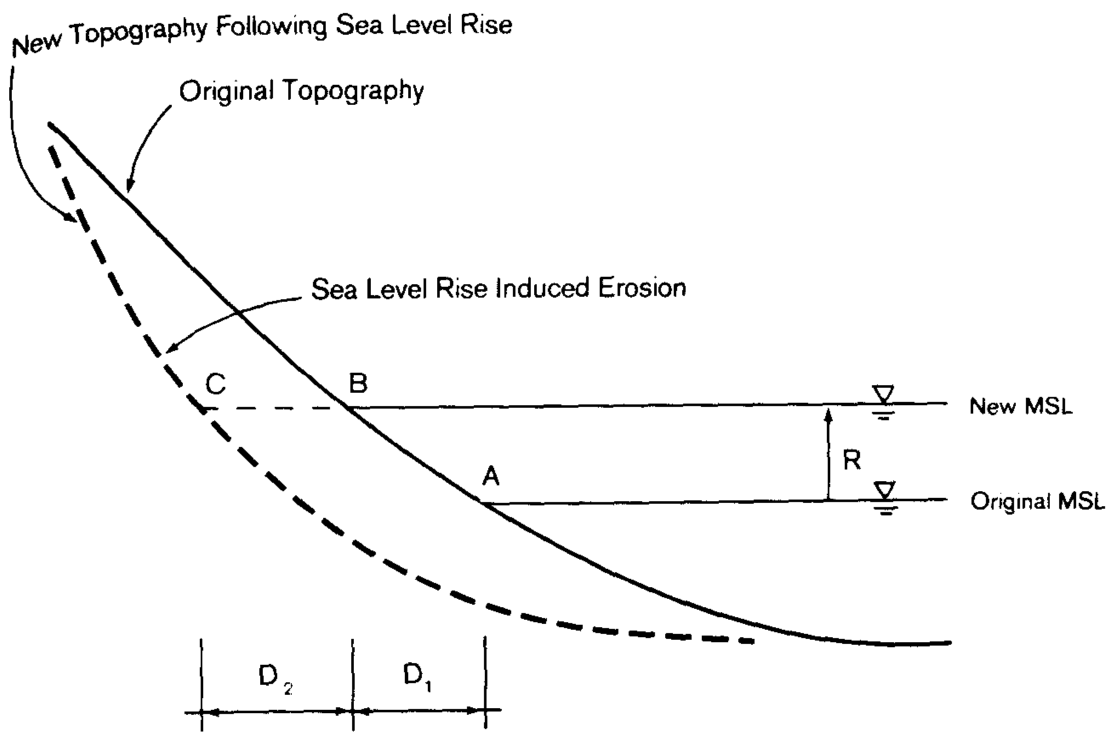

Figure 5-2. Shore adjustments with sea level rise.

Figure 5-2. Shore adjusements with sea level rise.

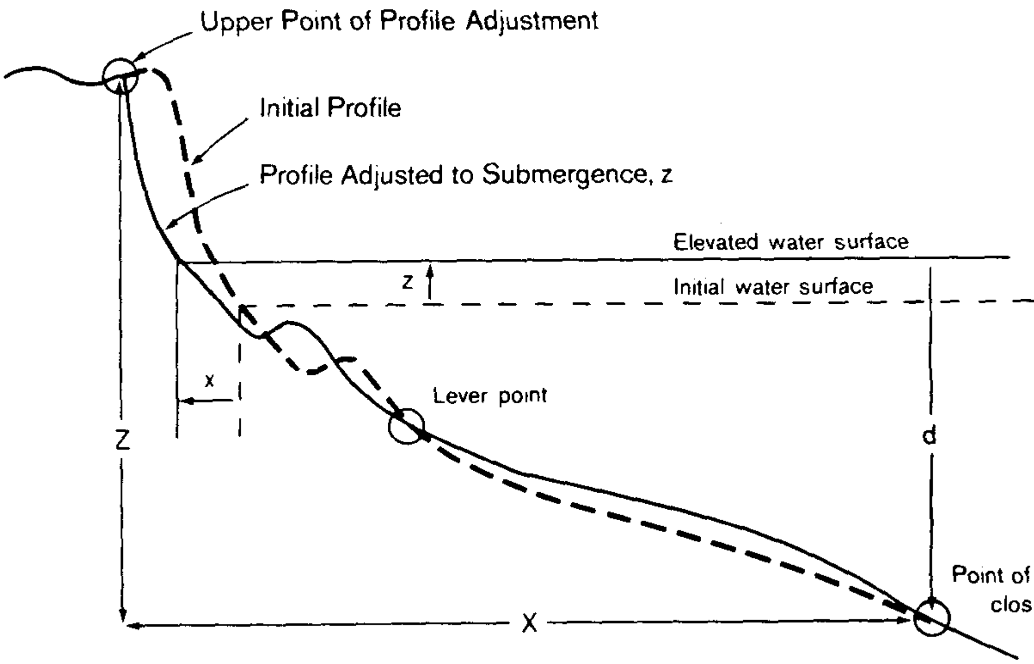

Figure 5-3. Shore adjustments to a change in water level elevation. *(After E. Hands, 1976, Predicting Adjustments in Shore and Offshore Sand Profile on the Great Lakes, CERC Technical Aid 81-4, Fort Belvoir, Va.: Coastal Engineering Research Center.)*

Figure 5-3. Shore adjustments to a change in water level elevation. *(After E. Hands, 1976, Predicting Adjustments in Shore and Offshore Sand Profile on the Great Lakes, CERC Technical Aid 81-4, Fort Belvoir, Va.: Coastal Engineering Research Center.*)

Methods

Two different approaches can be used to model shoreline reconfiguration in response to sea level rise. The Bruun Rule describes the equilibrium profile achieved after material removed during shoreline retreat is transferred onto the adjacent shoreface/inner shelf (Bruun, 1962; Weggel 1979; Schwartz and Fisher, 1979). The difficulty of defining the offshore limit of sediment transport limited the application of this procedure.

The second approach is less sophisticated for modeling purposes but more realistic in a geomorphic sense; it involves the empirical determination of new shorelines using trend lines. In this case, shoreline response is based on the historical trend with respect to the local sea level changes during that time period. This procedure accounts for the inherent variability in shoreline response based on differing coastal processes, sedimentary environments, and coastline exposures.

The method of projecting shoreline movement due to accelerated sea level rise is as follows. First, quantify historical shoreline movement for as long a period of record as possible (40 positions of shoreline change from 1850 to 1960 were tabulated in the study area). Second, establish a cm (ft) per year relationship for different shoreline types, wave exposures, and so on, using the historical rate of local sea level rise (Hicks et al.,1983). Last, determine a hypothesis or rule of thumb as the basis on which to project further sea level rise. In this case, shoreline movement relationships were selected, assuming that the amount of historical retreat is directly correlated with the rate of sea level rise. Therefore, a threefold rise in sea level will result in a threefold increase in the retreat rate, assuming lag effects in shoreline responses are small compared to overall extrapolation accuracy.

Tide gauge records document the relative (eustatic plus isostatic effects, such as subsidence) rate of sea level change over the period of record. The Galveston tide gauge records indicate that sea level rose about 18 cm (0.6 ft) between 1920 and 1960 (Hicks et al., 1983). A portion of this apparent rise was probably due to subsidence: 20 cm (0.6 ft) between 1943 and 1978. However, since no future subsidence is anticipated, the long-term (100 year) rate corresponds roughly to 30 cm (1 ft) per century. If only the 120-1940 record of sea level rise is considered, then the apparent rise would be 38 cm/100 years, of which it was estimated that 8 cm could be attributed to artificially induced subsidence. Using the longer-term data (1920-1960), a rate of 45 cm/100 years can be calculated, but at least 12 cm must be subtracted from this value because of subsidence. Therefore, an adjusted value of 30 cm/100 years has been utilized as the projected baseline sea level rise rate, since the actual amount cannot be exactly determined because of subsidence problems.

Historical shoreline data of mappable quality are available from 1850. The National Ocean Survey's (NOS, then called U.S. Coast Survey and U.S. Coast and Geodetic Survey) shoreline manuscripts were used for shoreline comparisons. The NOST sheets were made from field surveys and are the most accurate maps of the shoreline currently available (Shalowitz, 1964). Shorelines for 1850, 1930, and 1960 were delineated and utilized in the metric mapping procedure for map compilation.

The metric mapping technique is a system that emulates the best available photogrammetric techniques by making use of the data-manipulating capabilities of modern computers. This computer package includes simple transformations of original maps to state plane coordinates, space resection of photographs to correct inherent distortions, and a method for plotting data to produce final maps. The data are input through an X-Y coordinate digitizer (Tektronics digitizer, 0.005 in. accuracy) and finally drawn by a computer-driven plotter in order to provide a spatial depiction of historical shoreline changes. This method is the most accurate technique commonly used in coastal studies (Leatherman, 1983).

The shoreline change maps for the study area (Figure 5-1) indicate significant variations in response along the shore. The geologic/environmental resources map of the Galveston area (Fisher et al., 1972) was used to determine the geomorphic/substrate units (e.g., sandy deposits, marsh, spoil, and so on). Five shoreline types were differentiated: marsh; sandy beach/bluff; enclosed water body, no significant wave action; man-made shoreline, fill; and engineering structures, particularly rubble revetments, wooden bulkheads, concrete seawalls, groins, jetties, and dikes (levees).

For sandy shorelines with no development, the maximum rate of projected retreat was applied. For marsh shorelines, the historical rate of erosion represents a conservative value for the calculation of net excursion distance because marsh drowning was not considered. For shorelines that are partially protected by engineering structures, it can be assumed that the rate of shoreline retreat will be reduced, depending upon
stabilization efficiency. It should be noted that, although groins, where effective, limit longshore sediment transport by segmenting the shoreline, sand transport offshore (according to the Bruun Rule) with sea level rise can still occur. Also, groins will play little role in the abatement of shoreline recession where updrift sediment supply areas are absent or where little sand-sized material is actually being carried by the long. shore currents. Rubble toe protection is often only partially effective ill limiting erosion. This stabilizing process in effect only slows down shore retreat through time as new rubble is piled along the beach in ever more landward positions.

Results

Numerical values for shoreline change were calculated from the historical maps. For example, station 2 at San Leon, which is characterized by sandy clay material, has experienced 1.1 m (3.5 ft) of erosion per year from 1850 to 1960 (see Figure 5-4). The longer-term rate is a more accurate indicator of future changes except where subsequent engineering structures were certain to interfere with natural shoreline dynamics.

Future shore retreat was computed by multiplying the yearly averages by the number of years from present to the particular scenario year. Tables 5-2, 5-3, and 5-4 indicate the historical and projected shoreline changes for the various rise/rate combinations for the Galveston study area. In some cases, there are no anticipated shoreline changes due to human modifications. For example, along the Gulf Coast of Galveston Island (Figure 5-1), the shoreline is armored by a seawall erected in 1900. Therefore, no erosion is forecast for this area (see stations 34-40, Tables 5-3 and 5-4), since the beach is currently nonexistent and it was assumed that this massive engineering structure would remain intact.

In order to facilitate an economic analysis (see Chapter 7), the projected shoreline changes must be related to specific area losses. Therefore, the projected recession for the eight different combinations of rise per year were manually plotted to scale on the historical (base) maps. All four projected shoreline changes for a particular year (2025 or 2075) were plotted on the base maps. For example, in the map for San Leon (Figure 5-5), the present (1960) area of landmass is indicated by screening, and the subsequent predicted shoreline positions are shown by various dash and line patterns. If the high scenario rise rate is correct, then much of the community of San Leon will be lost because of shoreline retreat.

No shore accretion is forecast for Galveston Bay or the gulfside of Galveston Island for any of the scenarios. While the jetties at Bolivar Roads Inlet have been quite effective in trapping large quantities of sediment derived from littoral drift on north Galveston Island (Figure 5-6), this historical trend has now been reversed, since there is little updrift sand supply.(The beach in front of the Galveston seawall is nonexistent in many locations at present.) It is assumed that continued protection to the city of Galveston will be provided by raising the height of these structures as sea level rises.

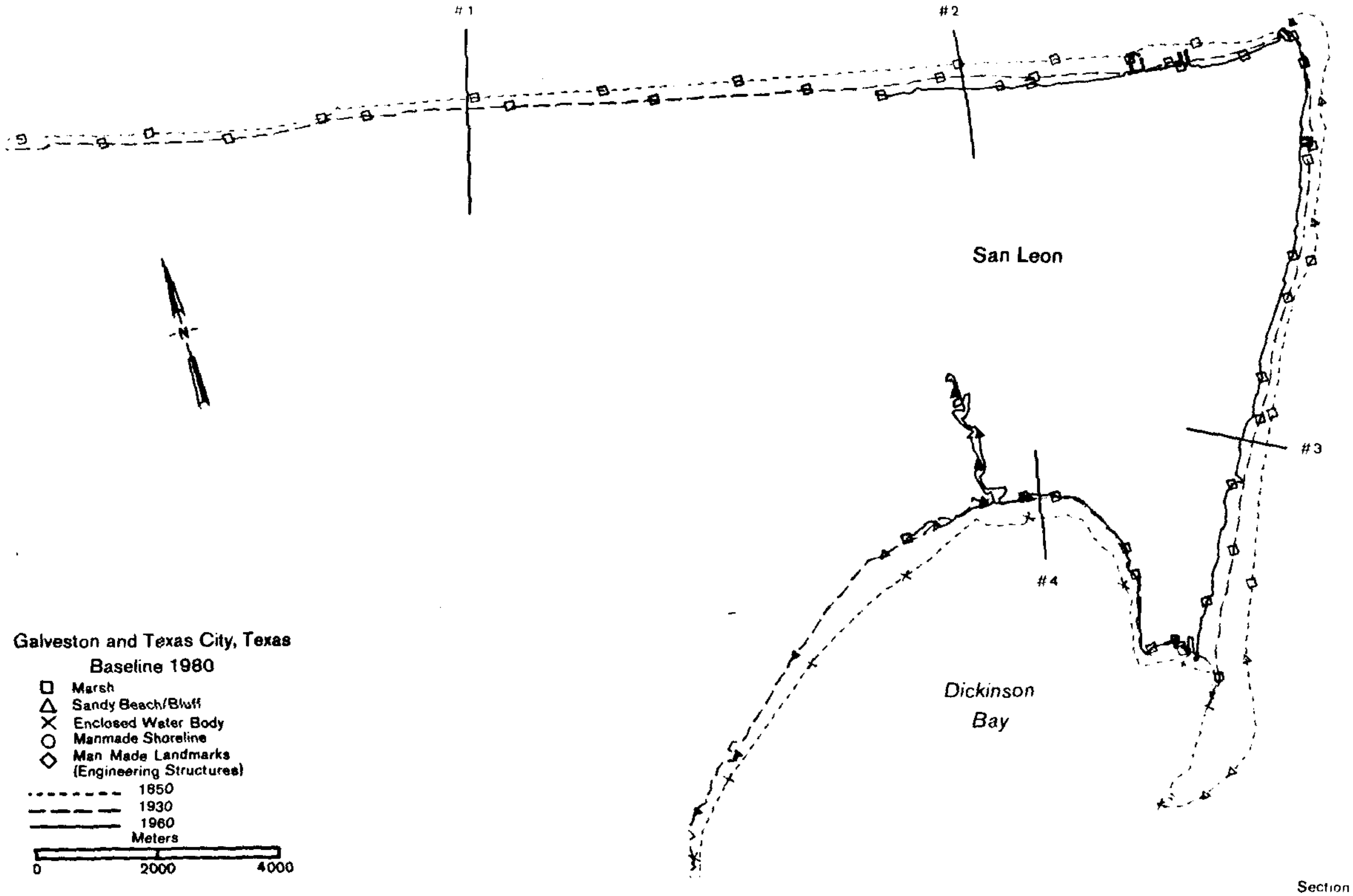

Figure 5-4. Historical shoreline changes, 1850-1960, Section 1.

Figure 5-4. Section 1. Historical Shoreline Shanges, 1850-1960,

Table 5-2. Historical Shoreline Changes, 1850-1960 (total recession in m)

		1850-1930		1930-1960		1850-1960		
Station	Material	Total	Rate	Total	Rate	Total	Rate	
1	Silt-clay	52	0.65[a]	-	-	-	-	
2	Sandy	64	0.80	61	2.03	125	1.14[a]	
3	Sandy	76	0.95	61	2.03	137	1.25[a]	
4	Silt-clay	101	1.26	15	0.51	116	1.05[a]	
5	Sandy	107	1.33	55	1.83	162	1.47[a]	
6	Silt-clay	76	0.95	52	1.73	128	1.16	0.0[a]
7	Marshy	24	0.31	-	-	-	-	0.0[a]
8	Marshy	6	0.08	24	0.81	31	0.28	0.0[a]
9	Marshy	34	0.42	3	0.10	37	0.33	0.0[a]
10	Marshy	43	0.53	3	0.10	46	0.42	0.0[a]
11	Sandy	92	1.14	55	1.83	146	1.33[b]	
12	Sandy	98	1.22	73	2.44	171	1.55[a]	
13	Sandy	52	0.65	61	2.03	113	1.03[a]	
14	Spoil	67	0.84	488[b]	-	421[b]	-	
15	Spoil	-	-	92[b]	-	-	-	
16	Marshy	40	0.50	21	0.71	61	0.55[a]	
17	Marshy	37	0.46	8[b]	-	29	0.26[a]	
18	Sandy	107	1.33	52	1.73	159	1.44[a]	
19	Sandy	79	0.99[a]	-	-	-	-	
20	Marsy	70	0.88[a]	-	-	-	-	
21	Silt-clay	67	0.84[a]	-	-	-	-	
22	Sand/spoil	168[b]	-	18[b]	-	186[b]	-	0.0[a]
23	Spoil	34[b]	-	3	0.10	31[b]	-	0.0[a]
24	Spoil	702[b]	-	0	0.00	702[b]	-	0.0[a]
25	Spoil	70[b]	0.00	45[b]	-	116[b]	-	0.0[a]
26	Spoil/bulkhead	397[b]	-	0	0.00	397[b]	-	0.0[a]
27	Bulkhead	28	0.34	0	0.00	28	0.25	0.0[a]
28	Spoil	-	-	122[b]	-	122[b]	-	0.0[a]
29	Marshy	64	0.80	15	0.51	79	0.72[a]	
30	Marshy	119	1.49	34	1.12	153	1.39[a]	
31	Sandy/spoil	-	-	76	2.54[a]	-	-	
32	Sandy/seawall	-	-	168[b]	-	-	-	0.0[a]
33	Sandy	-	-	122	4.07[a]	-	-	
34	Sandy/bulkhead	-	-	519[b]	-	-	-	0.0[a]
35	Sandy/jetty	1,373[b]	-	73[b]	-	-	-	1.0[a]
36	Sandy/seawall	183	2.29	9.2	0.31	192	1.75	0.0[a]
37	Sandy/seawall	70	0.88	0	0.00	70	0.64	0.0[a]
38	Sandy/seawall	122	1.53	0	0.00	122	1.11	0.0[a]
39	Sandy/seawall	198	2.48	89	2.95	287	2.61	0.0[a]
40	Sandy/seawall	305	3.81	24	0.81	329	2.99	0.0[a]

[a]Rate used in projection of shoreline change.
[b]Denotes accretion (in large part due to spoil deposition).

Table 5-2. Historical Shoreline Changes, 1850-1960, (total recession in m)

Table 5-3. Projected Shoreline Changes for 2025 (total recession in m)

Station	Descriptive Information	Baseline (13.7 cm)	Low (30.7 cm)	Medium (48.4 cm)	High (66.2 cm)
1	Groins	13	29	47	63
2	Groins	23	51	81	111
3	Groins	25	56	89	122
4	Groins	21	47	75	102
5	Fill	30	66	105	143
11	213m to dike	27	60	95	130
12	213m to dike	31	70	111	152
13	122m to dike	21	46	73	100
16	Marshy	11	25	40	54
17	Marshy	5	12	19	26
18	Sandy	29	65	103	141
19	Sandy	20	45	72	98
20	Marshy	18	40	64	87
21	Marshy	17	38	60	82
29	Marshy	15	32	51	69
30	Marshy	28	63	100	137
31	Marshy	51	114	181	248
33	Sandy	82	183	291	397

Note: Stations omitted where located along shoreline sections that have no projected changes.

Table 5-4. Projected Shoreline Changes for 2075 (total recession in m)

Station	Baseline (30.0 cm)	Low (92.4 cm)	Medium (164.5 cm)	High (236.9 cm)
1	62	188	335	481
2	108	327	583	839
3	119	360	642	925
4	100	303	540	777
5	140	424	756	1,087
11	126	381[a]	–[a]	–[a]
12	147	445[a]	–[a]	–[a]
13	98	296[a]	–[a]	–[a]
16	52	158	280	404[a]
17	25	76	135	194
18	137	415	740[a]	1,065[a]
19	94	285	508	730
20	84	255	454[a]	652[a]
21	80	242	432	622
29	68	206	367	528[a]
30	132	400[a]	713[a]	1,026[a]
31	241	730	1,301	1,873
33	387	-	-	-

[a]Indicates shoreline recession has proceeded to critical points, where further recession would result in the failure of a major structure.

Table 5-3. Projected Shoreline Changes for 2025 (total recession in m)

Table 5-4. Projected Shoreline Changes for 2075 (total recession in m)

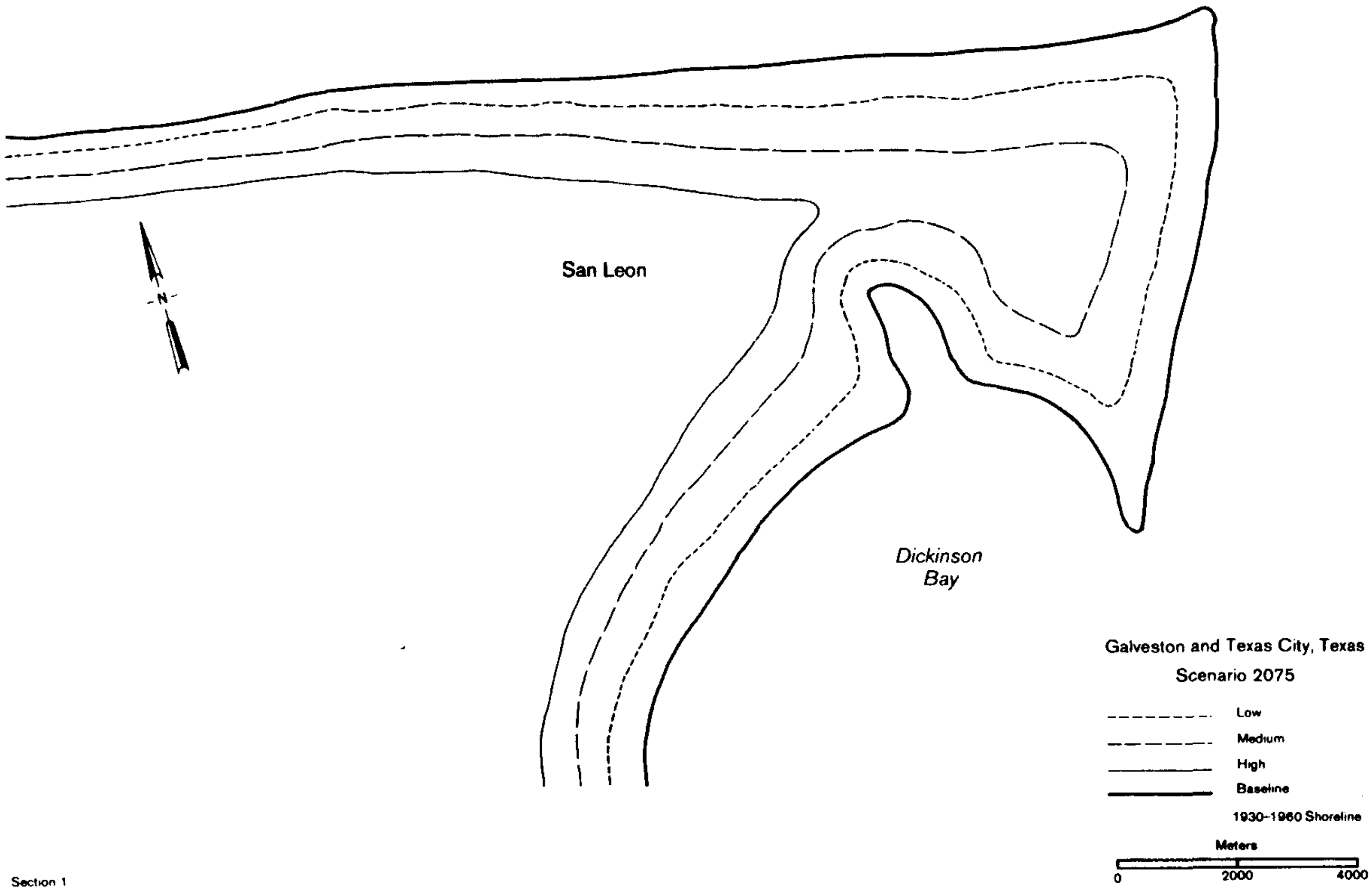

Figure 5-5. Projected shoreline changes in 2075 for four scenarios, Section 1.

Figure 5-5. Projected shoreline changes in 2075 for four scenarios, Section 1.

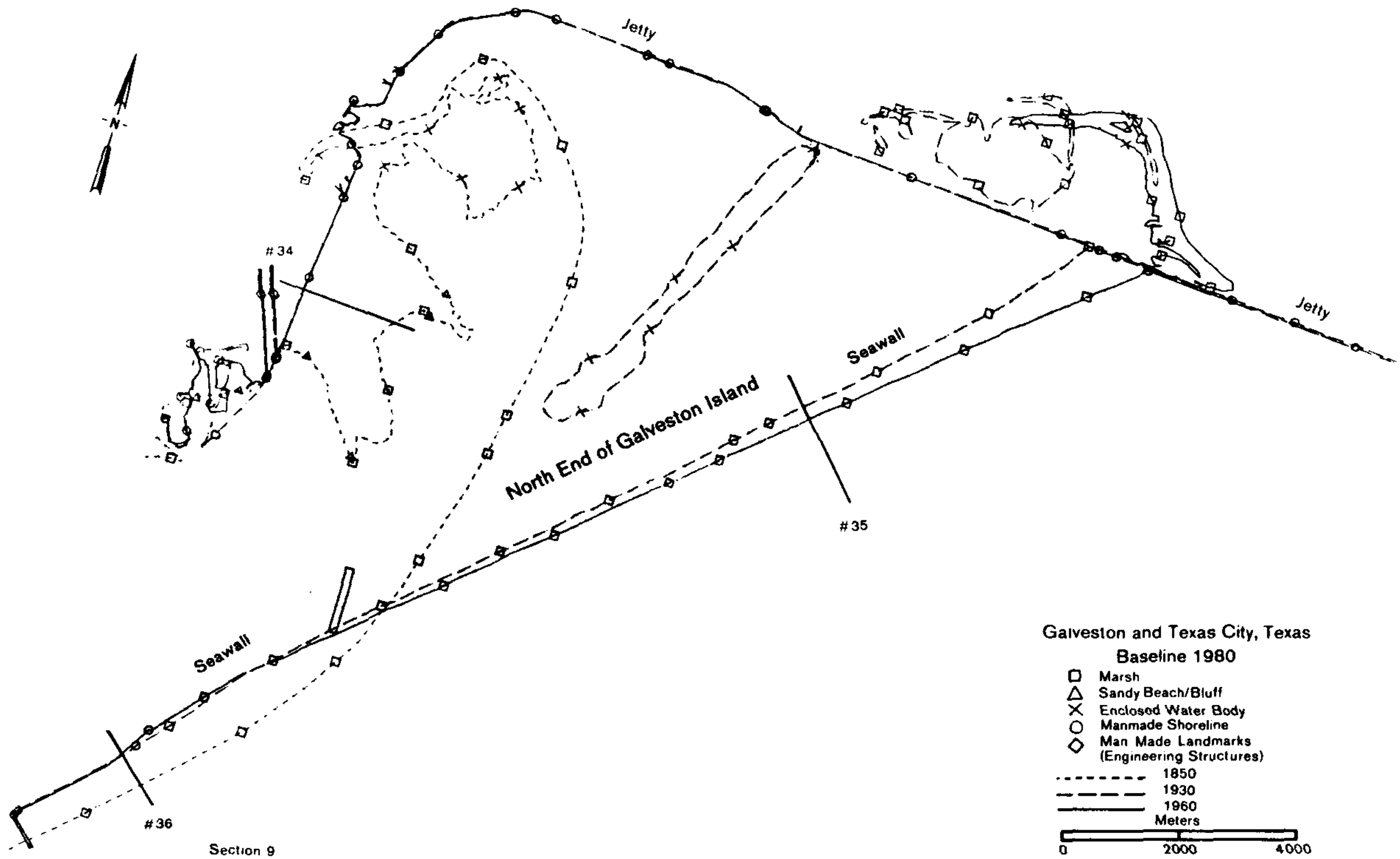

Figure 5-6. Historical shoreline changes, 1850-1960, Section 9.

Figure 5-6. Historical Shoreline changes, 1850 - 1960, Section 9.

Discussion

This type of analysis could be undertaken for any coastal plain shoreline. Microtidal bays and barriers are simpler systems to model than their mesotidal counterparts with large sediment inputs from riverine sources. The easily eroded unconsolidated sediments and gently sloping, low-lying topography make the projections straightforward, except where modified by coastal engineering structures. The underlying assumption of this analysis is that shorelines will respond in similar ways in the future, as was the case in the past, since sea level rise is the driving function and all other parameters remain essentially constant. With sea level rise, Galveston Bay will tend to deepen, but this trend will be largely offset because of deposition in accordance to the Bruun Rule and continued sediment input through Bolivar Roads Inlet.

It has been assumed that all substantial engineering structures will withstand failure. With the protective beach along the Gulf Coast of Galveston nearly depleted, the seawall becomes subject to undermining. Toe protection is being provided by large rubble blocks emplaced along the seaward edge of the Galveston seawall. With continued sand depletion, however, this rubble tends to "sink" to lower levels through time so that a second line of rubble has already been emplaced yet further seaward to protect that at the seawall toe. Hence, it is necessary to build structures to protect other structures, and this situation would be further aggravated by accelerated rates of sea level rise such that a further progression of these types of very expensive activities can be forecast in the future.

This analysis has assumed that total shoreline adjustments to sea level rise would be accomplished at the particular scenario year. Clearly, there will be some lag in shoreline response to higher water levels. It is possible that this time period will be on the order of 10-15 years, corresponding to the frequency of hurricanes with a storm surge level of 1. 5 m (5 ft). Since Galveston Bay depths are naturally less than 3 m (10 ft) and often less than 2 in (6 ft), a storm with such a surge would tend to overwhelm the system in comparison to the normal Bay tidal range of 0.15 m (0.5 ft) and accomplish a significant amount of the geologic work (erosion and deposition) necessary to restore profile equilibrium. Better information on storm frequency/magnitude would improve this analysis. Without site-specific data on many principal variables such as offshore profile *changes,* a simple extrapolation of historical trends is deemed the most reliable technique for forecasting shoreline changes.

STORM SURGE

Storm surges, the anomalously high tides produced by hurricanes and other coastal storms, are responsible for much of the damage in coastal areas as well as for extensive modification of the shoreline. The amount of damage to inland buildings and hazardous waste sites during storm conditions largely depends upon surge elevation and penetration. Sea level rise would alter storm surge levels in proportion to the amount of rise for any given scenario.

The Galveston Bay area is characterized by low-lying topography along a shallow, microtidal embayment. Sea level change will be particularly important in influencing this area, since the land is subject to flooding with even small rises. Also, storm surges superimposed on higher mean sea levels will tend to enhance shoreline erosion and bay sedimentation, as previously discussed.

Along the open coast, the amount of surge depends principally upon storm intensity and width of the continental shelf. The phase of the astronomical tide is also significant, since the coincidence of high tide and a storm surge would produce the highest storm tide (astronomical tide plus storm surge). Inland surge levels are highly variable and correspond to many variables, including basin shape and vegetation type. It is well known that surge height is amplified by funnel-shaped basins. Vegetation, particularly marshlands, attenuates the surge, since it is distributed as sheet flow over broad areas.

There are three sources of information on inland coastal storm surges: the Corps of Engineers' flood frequency curves, Federal Emergency Management Agency (FEMA) flood maps (FIRM), and the National Weather Service's SLOSH simulation computer model. Predictions of storm surge elevations are generally based on historical records of water levels occurring during previous storms. Frequency curves have been developed from a statistical analysis of tide gauge records and can be used to determine recurrence intervals for storms of particular sizes (Table 5-5). In some cases, the computation was based on frequency of central pressure indexes (U.S. Army Corps of Engineers, 1966).

Engineers and planners have established standard recurrence intervals to aid in the design of coastal engineering structures and in defining building setback lines, respectively. While various time periods have been utilized, the 100-year storm is used as the standard reference for flood elevation. A 100-year flood denotes that there is a 1 percent chance of occurrence in any given year. This definition does not imply that storms of this size will be spaced precisely 100 years apart because of the probabilistic nature of frequency magnitude relationships.-

Table 5-5. Frequency of Storm Tide Heights for Galveston

	Storm tide height above mean sea level	
Frequency (years)	*(ft)*	*(m)*
10	5.7	1.7
20	7.3	2.2
25	8.0	2.4
50	10.4	3.2
75	12.1	3.7
100	13.5	4.1
150	15.1	4.6

Source: From U.S. Army Corps of Engineers, Galveston District, 1966, "Texas City, Texas, Hurricane-Flood Protection," Design Memorandum no. 1, Hydrology, Galveston, Texas.

Table 5-5. Frequency of Storm Tides for Galveston

In addition to the surge frequency curves, 100-year flood maps by FEMA are available for most coastal communities. These flood insurance rate maps are essentially based on the storm surge frequency curve in combination with land elevations from U.S. Geological Survey topographic maps. The result is a map displaying the area subject to flooding during a 100-year storm. Areas so designed are further subdivided according to the potential damage, wherein the V zone corresponds to significant wave velocities encountered along the open coast. Recently, numerical storm surge models have been developed by the National Weather Service (Jelesnianski and Chen, 1983), and fortunately, Galveston Bay was one of the first areas so modeled by the National Hurricane Center using SLOSH.

Methods

The SLOSH model simulates wind speeds and storm surges based on meteorological conditions and surface characteristics (sea/bay bottom bathymetry and configuration, land elevation and morphology, and engineering structures such as jetties). This computer model numerically solves the equations of motion in order to determine surge height on a polar grid. The grid cells vary over the study area, but they are strategically placed so that the smallest cells are centered in Galveston Bay at 1.1 km (0.7 mi) spacing, with progressively larger cells being located in the Gulf of Mexico. Therefore, the polar grid permits greater accuracy (better resolution) in the more critical areas (Galveston Bay).

The SLOSH computer model yields a variety of data, but the most important in terms of storm damage functions are the composites of the storm surge envelopes that show maximum surge levels and penetrations on a grid cell basis. These surge values must have land elevations subtracted in order to yield surge penetration and height above mean sea level (see Figures 5-7 and 5-8). The three predicted flood levels corresponding to 15-20, 50-and 100-year storms have been computed for each grid square and are given in meters above mean sea level. For example, the block containing the G of Galveston (Figure 5-7) has a predicted surge of 1.5, 1.8, and 2.6 m for the three different sizes of hurricane.

The storm evacuation chart (scale of 1:62,500) by the National Ocean Survey (NOS) was utilized as the base map to overlay the transparencies by storm category. Category 3 storms (wind speeds of 11l-130 miles/hour and storm center barometric pressures of 950 mb) are roughly equivalent to the 100-year storm.[2] It should be noted that these hurricane categories are for "average" conditions, and no place along the coast is really average. Thus, the actual heights of the storm tide for the 100-year storm at Galveston will exceed this table value (Table 5-5), since the surge is increased because of site-specific conditions (particularly the gentle offshore/nearshore sloping bottom). Category I storms (which are estimated to be 15-year storms) are the most frequently occurring event that results in significant damage. Note that the use of return intervals is somewhat subjective, since only short-term, high quality historical records are available. The 1900 hurricane, which devastated Galveston Island, was a category 3 or 4 storm; the poor quality of the available meterological data limits a precise definition of its intensity.

Over 77 separate simulations were run with the SLOSH model, based on variations in hurricane approach direction, storm speed, and differences in storm intensity along the pathway. The maximum storm surge value for each grid cell was obtained by determining the envelope for all surge overlays. The computed surges are estimated to be within 20 percent of the observed water levels (Ruch, 1981).

In interpreting the SLOSH data, the following precautions must be kept in mind: (1) integrity of the Texas City levee system and Galveston seawall is assumed; (2) no adjustments have been made for wave action that could overtop the levee and/or seawall; (3) no adjustments have been made for possible flooding by hurricane-generated rainfall behind the levee or seawall; and (4) the entire area could possibly be flooded during intense hurricanes without overtopping because of surge penetration from unprotected flanks of Texas Cit and bayside of Galveston Island (Ruch, 1981).

In order to determine the storm surge levels with accelerated sea level rise, the particular value for a year/rise combination was added to the predicted surge levels for the three storm sizes. For areas already subject to flooding, this approximation would yield a conservative value for heightened flooding, since the boundary conditions, particularly the area for storm surge ingress, were invariant. Where the SLOSH results yielded zero values for protected areas, this value was not altered unless the flood waters overtopped the threshold elevation. In this case, the algebraic sum of the maximum storm values derived by the numerical model (SLOSH) at the grid point nearest the protective structure (e.g., levee, seawall) and the height values for a particular scenario/year were used calculate the flooding value. Since grid cell values are based on composite values from 77 computer simulation runs, it would be time and cost prohibitive to consider running this set by SLOSH for the 8 rise/year combinations (77 x 8 total permutations to calculate the maximum, envelope of envelopes) to yield the actual values.

The present maximum storm surge levels predicted for 15-, 50-, and 100-year storms are shown for the city of Galveston and Texas City in Figures 5-7 and 5-8, respectively. For the SLOSH model, it was assumed that all coastal engineering structures remained intact during storm conditions and there was essentially no leakage (note zero values for the two urban enclaves). This may not be a good assumption for the Texas City levee system because this earthen structure has already been drawn close to the shore in several areas by pervasive ongoing erosion. The surge values for two small water bodies surrounded by the Texas City levee are in situ storm surge due to wind set-up. Values from Table 5-1 were used to determine the level of increased flooding due to sea level rise for areas already flooded during a particular size storm. Areas currently not flooded by a particular size storm are protected by a coastal engineering structure, such as a seawall or levee. Once the floodwaters overtop these structures, then the protected areas are subject to the same level of flooding as adjacent, nonprotected areas, provided that there is enough time to pour water over the "lip" of the structure to fill the "basin." Since the storm surge peak will only last a few hours, there may not be enough time to fill the basin, depending upon its size, the depth of overflow, and the perimeter length over which a particular depth of water is overtopping.

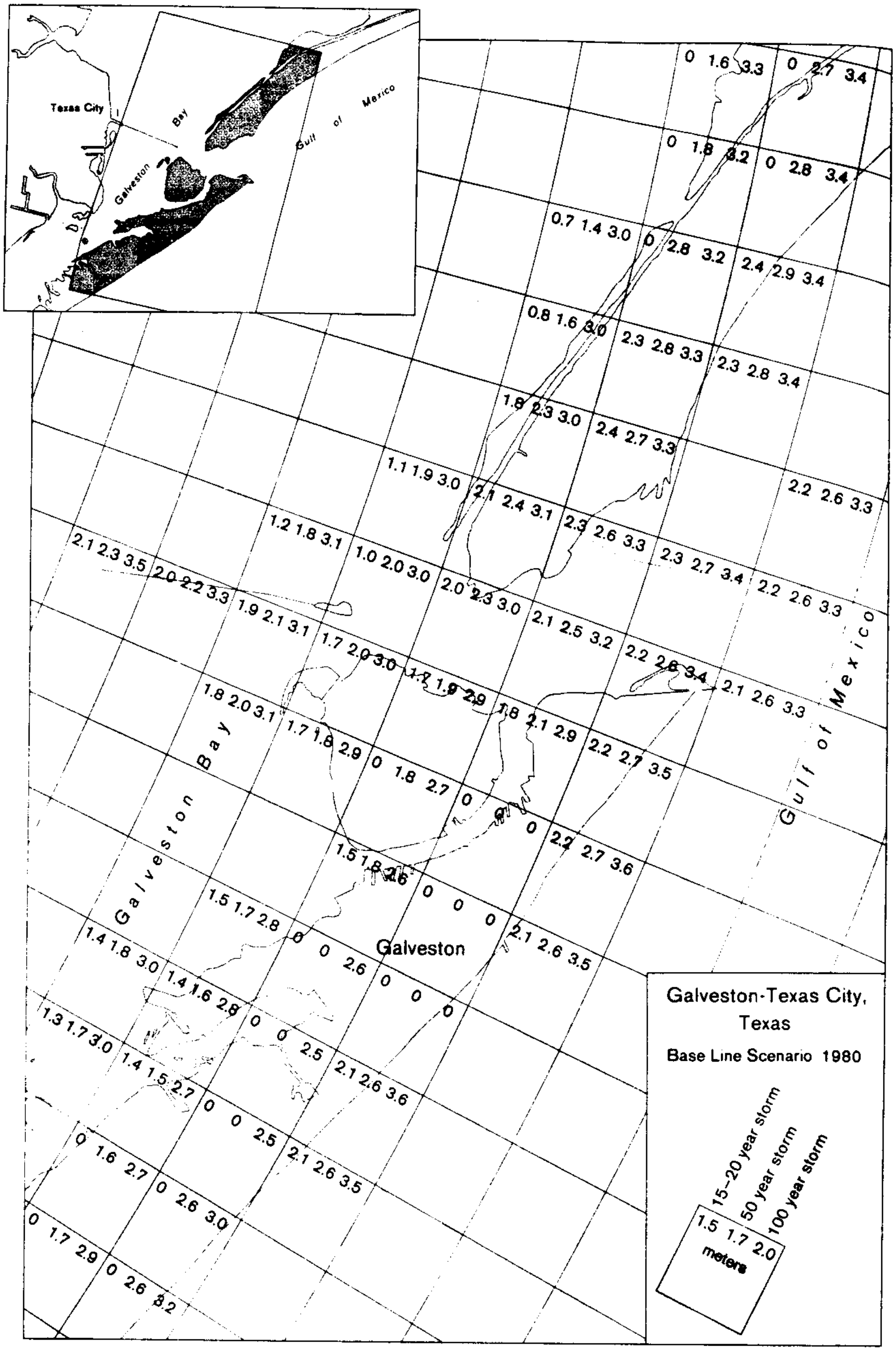

Figure 5-7. Storm surge levels for Galveston, baseline scenario, 1980.

Figure 5-7. Storm surge levels for Galveston, baseline scenario, 1980.

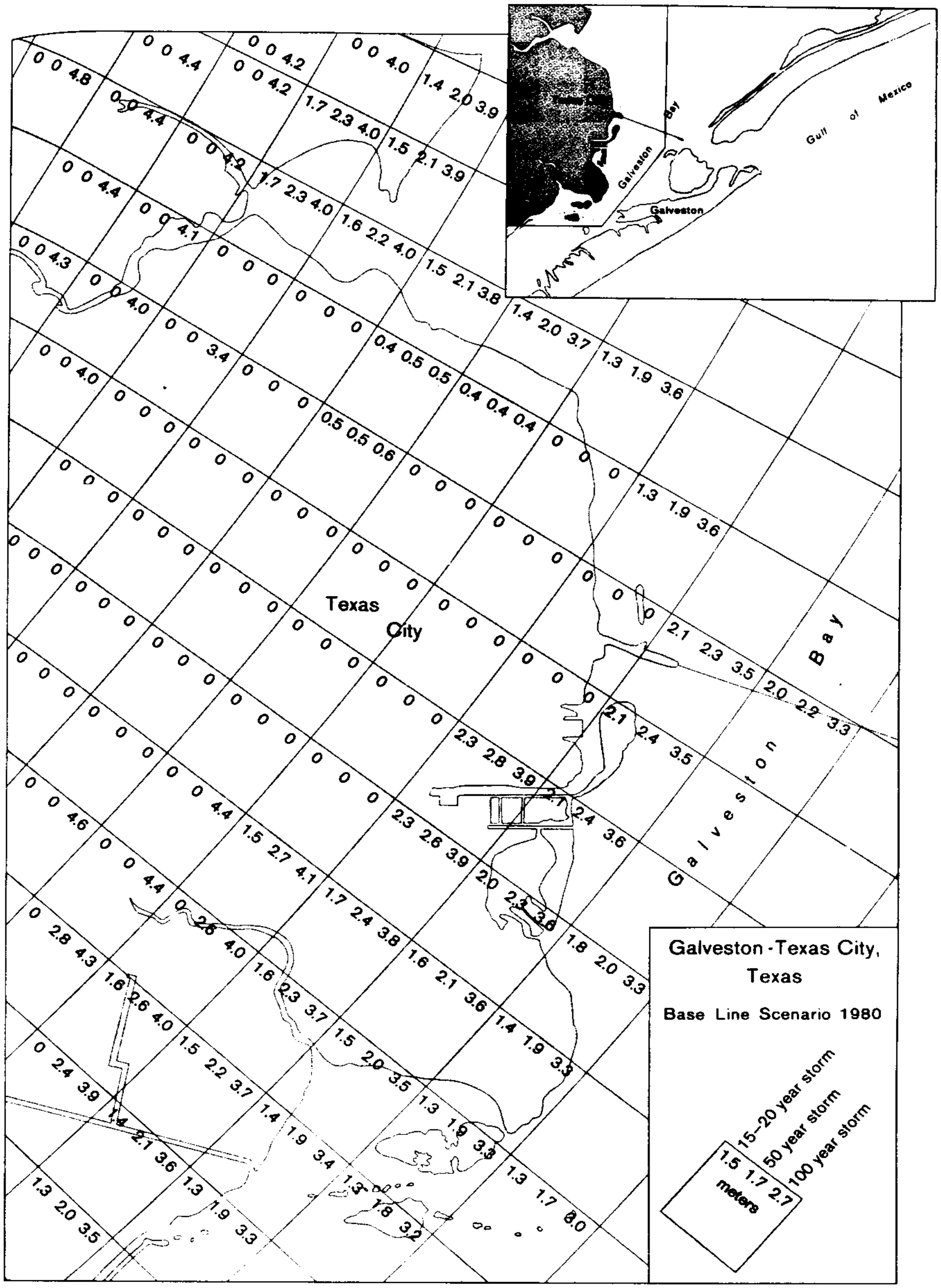

Figure 5-8. Storm surge levels for Texas City, baseline scenario, 1980.

Figure 5-8. Storm surge levels for Texas City, baseline scenario, 1980.

Galveston is subject to flooding along much of the bayside and the city is quite small in area; therefore, Galveston city would be flooded to the maximum extent possible. In the case of Texas City, flooding can often occur from both the north and south flanks. While Texas City covers a much larger area, its defenses to flooding, principally the levee system, are largely, composed of earthen materials and are, subject to collapse under attack by even a 50-year storm for the high scenario sea level conditions. Considering these factors, Texas City would also be flooded to the maximum extent possible once the limiting elevational criterion for flooding was exceeded.

Table 5-6. Storm Surge Flooding with Sea Level Rise for Protected Urban Areas

Table 5-6. Storm Surge Flooding with Sea Level Rise for Protected Urban Areas

Location	*Storm (years)*	*Year*	*Scenario*	*Storm Surge m*	*ft*
Texas City	100	2075	High	6.5	(21)
Texas City	100	2075	Medium	5.8	(19)
Texas City	100	2075	Low	5.0	(16)
Texas City	100	2025	High	4.7	(15)
Texas City	50	2075	High	5.0	(16)
Texas City	50	2075	Medium	4.3	(14)
Galveston	100	2075	High	5.8	(19)
Galveston	100	2075	Medium	5.2	(17)
Galveston	100	2075	Low	3.7	(12)
Galveston	100	2025	High	3.4	(11)
Galveston	50	2075	High	5.0	(16)
Galveston	50	2075	Medium	3.5	(11)
Galveston	15	2075	High	4.4	(14)
Galveston	15	2075	Medium	3.4	(11)

Results

Table 5-6 summarizes the results of this analysis and indicates the depth of flooding for each area according to storm size and scenario/year combinations. The surge values for the entire study area have also been computed on a grid cell basis (Leatherman et al., 1983).

In the case of Texas City for a 100-year storm in 2075, flooding resulted from water rushing over low elevation areas along both the north and south flanks (see Figure 5-9). Along the north flank, the Southern Pacific Railroad tracks serve as a dike with an average maximum elevation of 3.4 m (11 ft). The floodwaters would reach this area via Dickinson Bayou in large quantities. Bayou Vista on the south flank of Texas City has a maximum continuous elevation of 4.6 m (15 ft). In all cases, the levee system along Galveston Bay, which ranges in elevation between 6.4 and 7.0 m (21-23 ft), served as a total barrier to the storm surge. Although the floodwaters, without consideration of the superimposed storm waves, would nearly reach the top of the levee, structural continuity of this coastal engineering structure was assumed.

Texas City would be subject to flooding during a 50-year storm in 2075 under the medium or high scenarios. In the case of the medium scenario, flooding would result from overtopping along the north flank only. Except for the six cases shown in Table 5-6, the water was held back by the protective devices, assuming no structural failure, and the surge values will be zero in the protective enclaves.

A similar analysis was conducted for Galveston city. Its seawall has an average elevation of 4.9 m (14 ft), effectively restraining floodwaters below this value. Along the bay side of Galveston, the elevation varies greatly, ranging as low as 1.5 m (5 ft) to over 3 m (10 ft). While the bayside piers could be flooded under almost all conditions, it was assumed that the 3 m (10 ft) elevation was the threshold value for the flooding of downtown Galveston city. In three cases, Galveston was flooded by ocean overtopping of the seawall (2075; 100-year storm, high and medium scenarios; and 50-year storm, high scenario) as well as bayside flooding. Figure 5-10 illustrates storm surge levels for the medium scenario in 2075. In the case of oceanside flooding, it must be realized that the water is overflowing the seawall and attacking the city buildings with force because of the intensity of breaking storm waves from the deep ocean. In all other cases, flooding occurred from the bay side as the storm surge entered Galveston Bay through Bolivar Roads Inlet.

Table 5-6 is instructive in terms of planning, since it appears that the probability of damage is weighted toward the 2075 time period after sea level rise has appreciably elevated the water height. Also, the larger magnitude storms, particularly the 100-year event (class 3 hurricane), are the greatest threat in terms of flooding regardless of the particular scenario. For example, a 100-year storm can result in the flooding of both Galveston and Texas City by 2075, assuming even the low sea level rise scenario (Table 5-6).

The effect of sea level rise can also be considered in another way; the addition of even small amounts of water (sea level rise) can considerably change the storm size according to frequency (Table 5-5). The frequency of storm tide heights for Galveston Bay is based on historical records of high water levels compiled by the U.S. Army Corps of Engineers (1966). Table 5-5 represents the recurrence intervals for particular flood levels that have been statistically determined from these measurements. The general results for the entire Galveston area agree fairly well with the area-averaged values obtained from numerical modeling (Figures 5 -7 and 5-8). In general, these data indicate that the 0.4 in (1.3 ft) rise in sea level associated with the medium scenario in 2025 would convert a 75-year storm into a 100-year storm (Table 5-5). Likewise, if the high scenario proved to be correct, then the flooding associated with a 100-year storm would occur at only a 10 year frequency by 2075, resulting in catastrophic damage to the study area. Also, many zones now outside the 100-year floodplain would be flooded by a 75-year storm. The potential destruction by these storm floods would significantly increase, since damage depends upon surge level.

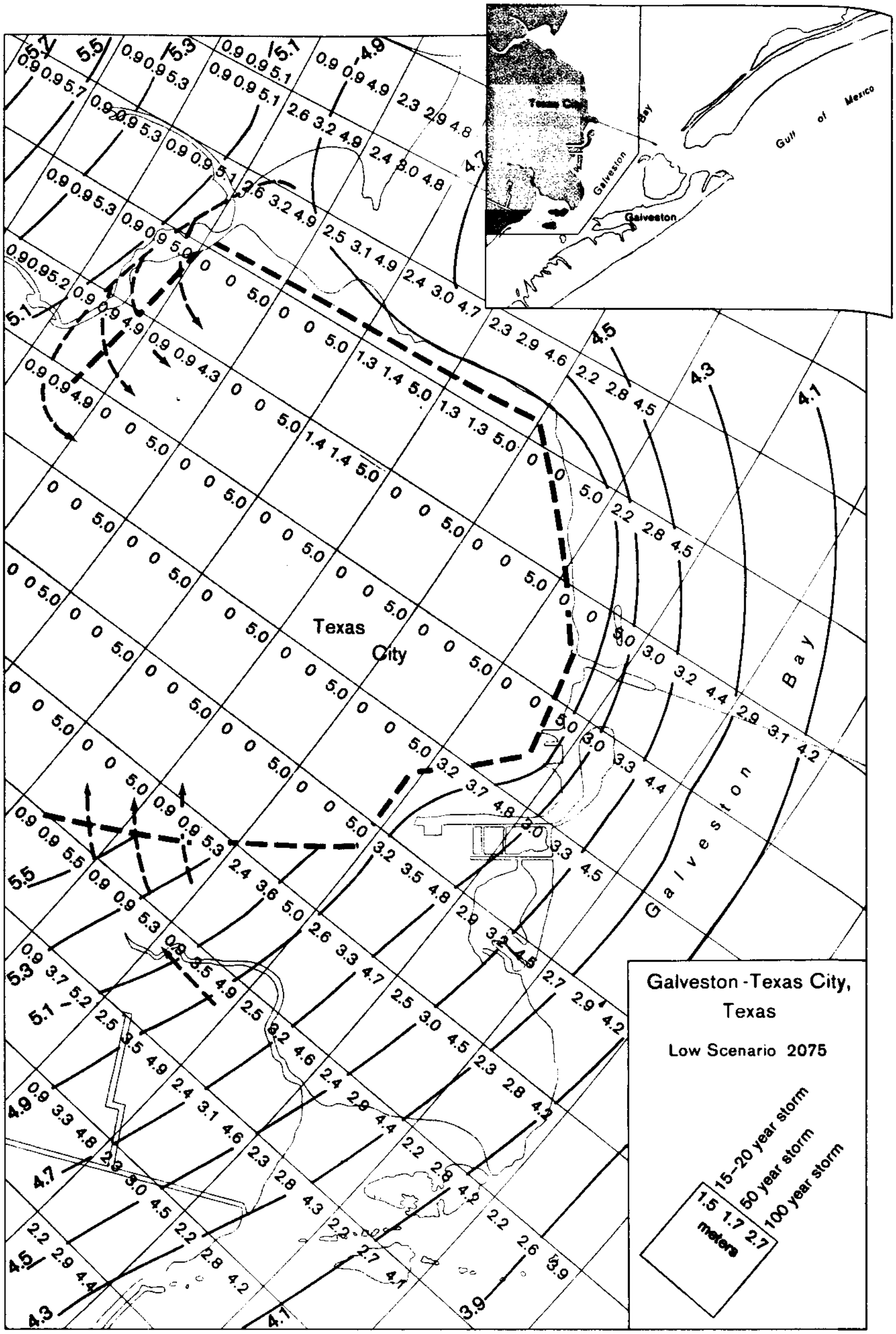

Figure 5-9. Storm surge levels for Texas City, low scenario, 2075.

Figure 5-9. Storm surge levels for Texas City, low scenario, 2075.

Discussion

It is clear from the surge heights that the shape of Galveston Bay serves to amplify surge magnitude (Figures 5-7 and 5-8). In fact, open bays, particularly funnel-shaped estuaries, tend to increase the storm surge, resulting in higher water levels during storms than those on the adjacent open coasts (Reid and Bodine, 1968).

While sea level rise would result in some modifications in bay shape and inlet configuration, these effects are too small to result in a significant change in storm surge modeling, considering the scale of the grid cell: 1.1 km (0.7 mi). Also, the storm surge analysis does not include any effects of shoreline change. Exact shoreline position is not really a factor in this analysis, considering the fact that only large-scale features are important with such a coarse grid.

There is no reason to anticipate significant alterations in major land forms due to storm surges with low levels of sea level rise by the year 2025 (except possibly for the high scenario). Galveston Bay has experienced storm surge water levels that greatly exceeded this level during this century, most notably the 1900 hurricane. With a 2.3 m (7.8 ft) rise in sea level (Table 5-1), however, modification of the shorelines of the outlying barrier islands could possibly be so drastic as to significantly alter storm surge levels. In particular, the southern end of Bolivar Peninsula could be essentially submerged or beveled (eroded) sufficiently to increase dramatically the hydraulic radius (cross-sectional area divided by the wetted perimeter) of the Bolivar Roads Inlet during storm conditions. This could greatly increase the height of the storm surge in Galveston Bay. Considerable study, however, would have to be devoted to this topic in order to determine the evolutionary characteristics and responses of low elevation landform features to such rapid rates of rise and drastic levels of the sea.

While the FEMA flood maps in conjunction with the storm frequency curve and topographic maps could have been used to yield some indication of storm surge levels, the SLOSH numerical model yields far more reliable results and allows for predictions on a grid-cell basis rather than a single averaged value for the entire basin. The National Weather Service is planning to model all the significant basins along the U.S. Atlantic and Gulf coasts, but the dates of completion for particular areas range from years to decades. This type of analysis can be utilized for any area so modeled. It should be noted that there is a fairly wide band in predicted values (accuracy within 20 percent of true value) so that ranges are more appropriate than absolute values for characterizing a storm surge.

CONCLUSIONS AND RECOMMENDATIONS

Large-scale engineering works (e.g., the Galveston seawall and Texas City levees) have been constructed to protect urban complexes on the basis of existing water level, tide, and wave energy criteria. Therefore, their resistance to failure is predicated on present conditions existing, into the foreseeable future, which generally translates to a projected 100-year lifetime for most Corps of Engineers projects. It should be note that problems have already developed along the Galveston seawall due to sand depletion, and shore erosion will soon threaten sections of the Texas City levee.

Major benefits from correctly forecasting sea level rise can be considered for two contrasting situations: undeveloped in contrast to urbanized shore. Where the land adjacent to the Gulf or Galveston Bay is undeveloped, then future facilities should be located far inland in order to avoid direct undermining with shore retreat. Building setback lines should be based on the projected shoreline positions due to accelerated sea level rise rather than a straight line extrapolation of historical trends. Also, buildings on low-lying terrain not subject to erosion will have to be placed on much higher pilings, with the height corresponding to the total rise in sea level.

Where the land is already highly urbanized, a different strategy should be advanced. Where feasible, industry should be located further inland over the longer term, instead of refurbishing old buildings. Where portside location is essential to the conduct of business, engineering structures should be built to withstand stresses generated by major storms arriving superimposed on elevated water levels. One approach is to

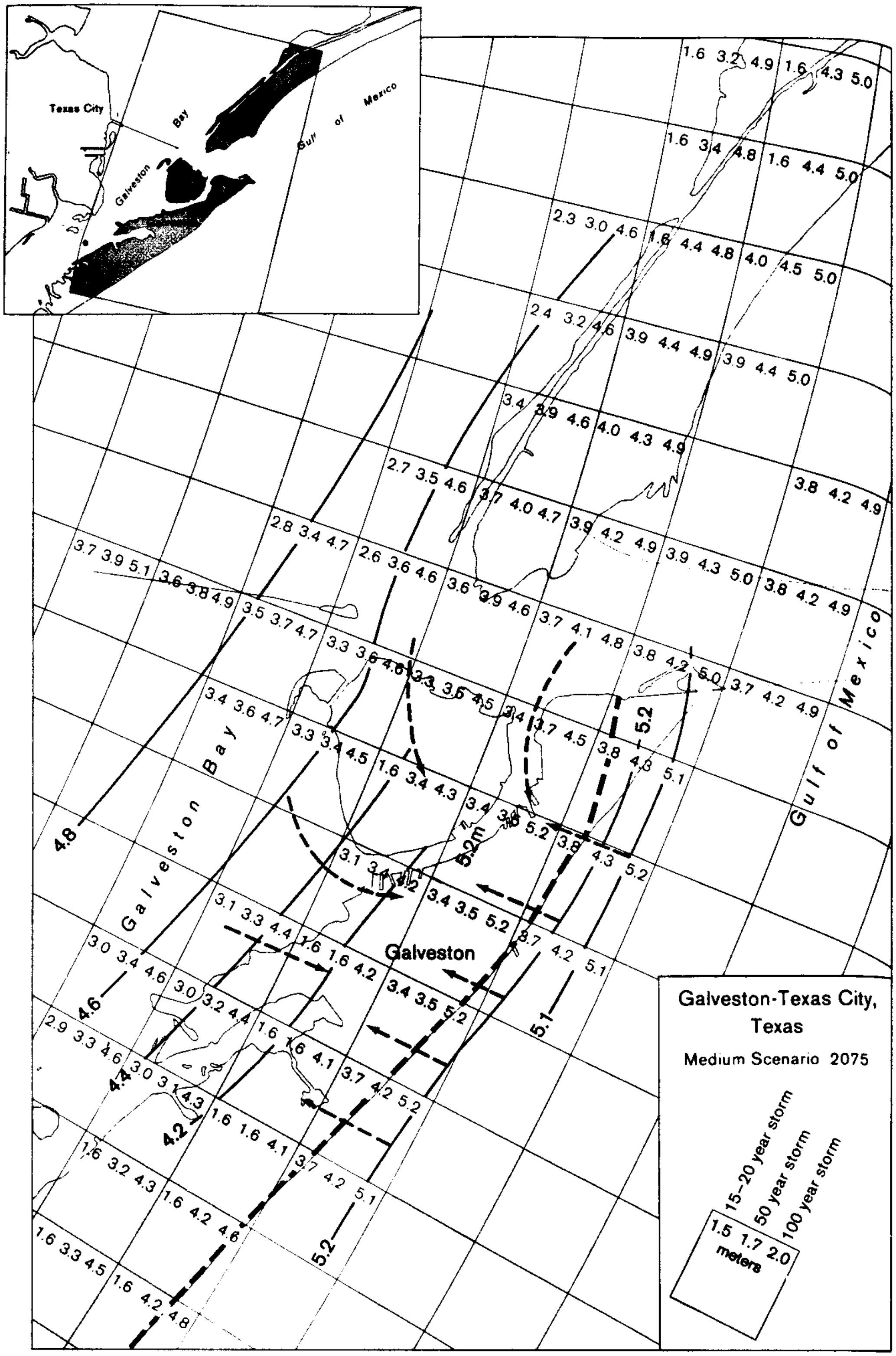

Figure 5-10. Storm surge levels for Galveston, medium scenario, 2075.

Figure 5-10. Storm surge levels for Galveston, medium scenario, 2075.

construct heavy duty bases so that lifts can be added in the future to provide elevational adjustments in accordance with sea level rises. If basal structures are not engineered to these more rigid specifications, then the entire protective device may be ineffective during more severe conditions in the future and may not possess the strength to withstand the top-loading and reinforcement that would eventually be necessary.

In general, the principal strategy that should be employed along developed shores in the face of rising seas will involve fortressing small urban enclaves. Fortified levee and dike systems with movable locks encircling all critical facilities will prevent storm surge flooding. These fortifications will have to be well engineered to provide structural continuity.

The other alternative, which has already been suggested by the U.S. Army Corps of Engineers (1979), is to seal off the entire Galveston Bay area during storm attack. This procedure is being utilized to protect London with large movable gates that can close off the Thames River to ocean waters. After the 1938 hurricane, gates that function in a similar manner were installed along the upper part of Narragansett Bay to protect Providence, Rhode island, from future stormwater damage. Where high relief terrain exists, such as along the glaciated New England coast, or in narrow sections that necessitate blockage, this approach will be acceptable. The suggestion has been made to emplace such a structure at the Bolivar Roads Inlet, but the cost is, at present, prohibitive and the success uncertain. In order for this type of protective device to be effective, there must be no "holes" in the dike/dam system. While the inlet gate may be made secure, the low-lying barrier islands to either side must remain intact for many miles in either direction. The higher projected rates of sea level rise may result in the partial dissolution of these barrier islands. In any case, the length of dike that would have to be maintained virtually precludes this alternative from future consideration for the Galveston area.

NOTES

1. William Seelig, 1982, Waterways Experimental Station, Vicksburg, Miss., personal communication.
2. Jarvinen, R., 1982, National Hurricane Center, personal communication.

REFERENCES

Bird, E. C. F. 1976. "Shoreline Changes during the Past Century." In *Proceedings of the 23rd International Geographical Congress,* Moscow: IGC.

Bruun, P. 1962. "Sea Level Rise as a Cause of Shore Erosion." Journal *of the Waterways and Harbors Division* 88(WW1):117-130.

Fisher, W. L., J. H. McGowen, L. F. Brown, Jr., and C. G. Groat. 1972. *Environmental Geologic Atlas of the Texas Coastal Zone: Galveston-Houston Area.* University of Texas-Austin: Bureau of Economic Geology.

Hands, E. B. 1976. *Predicting Adjustments in Shore and Offshore Sand Profiles on the Great Lakes.* CERC Technical Aid 81-4. Fort Belvoir, Va.: Coastal Engineering Research Center.

Hicks, S. D., H. A. Debaugh, Jr., and L. E. Hickman, Jr. 1983. *Sea Level Variations for the United States, 1855-1980.* NOAA report. Rockville, Md.: NOAA.

Jelesnianski, C. P., and J. Chen. 1984 (in press). *SLOSH (Sea, Lake, and Overland Surges from Hurricanes).* NOAA technical memorandum. Silver Spring, Md.: NOAA.

Leatherman, S. P 1983. "Shoreline Mapping: A Comparison of Techniques." *Shore and Beach* **51**:28-33.

Leatherman, S. P., M. S. Kearney, and B. Clow. 1983. *Assessment of Coastal Responses to Projected Sea Level Rise: Galveston Island and Bay, Texas.* URF report TR-8301; report to ICF under contract to EPA. College Park: University of Maryland.

Reid, R. O., and B. R. Bodine. 1968. "Numerical Model for Storm Surges in Galveston Bay." *Journal of the Waterways and harbors Division* **94**(WW1):33-57.

Ruch, C. 1981. *Hurricane Relocation Planning for Brazoria, Galveston, Ha*rris, *Fort Bend and Chambers Counties.* Texas A&M University Sea Grant report 81-604. College Station, Tex.: Texas A&M University.

Schwartz, M. L., and J. J. Fisher, eds. 1979. *Proceedings of the Per* Bruun Symposium. Newport, R.I.: IGU Commission on the Coastal Environment.

Shalowitz, A. L. 1964. *Shore and Sea Boundaries.* Vol. 2. Department of Commerce Publication 10-1. Washington, D.C.: Government Printing Office.

Thompson, R. E. 1982. *Subsidence '82: Harris-Galueston Coastal Subsidence District.* Houston, Tex.: Estey Houston and Associates.

U.S. Army Corps of Engineers, Galveston District. 1966. "Texas City, Texas, Hurricane-Flood Protection." Design Memorandum 1, Hydrology. Galveston, Texas: U.S. Army Corps of Engineers.

U.S. Army Corps of Engineers, Galveston District. 1979. *Texas Coast Hurricane Study: Galveston Bay Study Segment.* Galveston, Tex.: U.S. Army Corps of Engineers.

Weggel, R. 1979. A *Method for Estimating Long-Term Erosion Rates* from a *Long-Term Rise in Water Level.* CERC Technical Aid 79-2. Fort Belvoir, Va.: Coastal Engineering Research Center.